Interface roughening of Ge δ layers on Si(111)

J. Falta, T. Gog, and G. Materlik
Hamburger Synchrotronstrahlungslabor (HASYLAB) am Deutschen Elektronen-Synchrotron DESY, Notkestrasse 85, 22607 Hamburg, Germany

B. H. Müller and M. Horn-von Hoegen
Institut für Festkörperphysik, Universität Hannover, Appelstrasse 2, 30167 Hannover, Germany
(Received 23 September 1994; revised manuscript received 5 December 1994)

Ge δ layers, grown by molecular-beam epitaxy (MBE), surfactant-mediated epitaxy, and solid-phase epitaxy were characterized *in situ* by high-resolution low-energy electron diffraction and post growth by x-ray standing waves. Initial growth of Ge on Si is found to proceed in a double-bilayer fashion. Subsequent Si deposition leads to a bilayer growth mode. MBE Si deposition is accompanied by Si-Ge site exchanges leading to increased interfacial roughening, which can be partially reduced by solid-phase epitaxy and use of surfactants.

I. INTRODUCTION

Fabrication of ultrathin (≤ 1 nm) heterostructures (δ layers) for semiconductor devices is an important goal in material science. It may open new possibilities for device design such as high-speed resonant tunneling or optical devices, based on Si technology. With decreasing device dimensions, the crystalline quality of films and the abruptness of the interfaces will become crucial for device quality and electronic properties.

Structural characterization of buried δ layers with a thickness smaller than 1 nm is a difficult task. Secondary-ion mass spectrometry (SIMS) and cross-sectional transmission electron microscopy (XTEM) are common tools for thin-layer characterization. Depth resolution of SIMS is limited to ~ 5 nm.[1] XTEM allows observation of atomic structures; however, despite recent progress in data evaluation,[2] chemical sensitivity is limited. Rutherford backscattering spectrometry[3] (RBS) from ions and medium-energy ion scattering[4] (MEIS) of buried layers is limited intrinsically in depth resolution due to energy straggling effects: The best achievable resolution is ~ 1 nm.[5] Electron spectroscopical methods, like Auger spectroscopy, x-ray photoemission spectroscopy (XPS), and ultraviolet photoelectron spectroscopy (UPS) are element specific, but spatial resolution is limited due to a finite escape depth of electrons. Measurements of high spatial resolution are possible by high-resolution x-ray diffraction (HRXRD) and interesting results[6] have been obtained by combined studies with HRXRD and x-ray standing waves (XSW).

Here we present an alternative approach by combination of spot profile analysis of low-energy electron-diffraction (SPALEED) characterization during growth and post-growth x-ray standing-wave measurements of buried δ layers. SPALEED is sensitive to steps of the growth front and, therefore, provides information on film morphology during growth. XSW is element specific and extremely site sensitive, with achievable resolution in the order of 0.01 Å.[7] In this study, SPALEED was used to deduce the Ge morphology during Ge growth. XSW measurements were performed to investigate changes of interface morphology due to growth of a top Si buffer layer.

This study presents characterizations of Ge δ layers with Ge layer thickness ranging from 0.5 to 1.5 BL [1 bilayer (BL) $= 15.6\times10^{14}$ cm^{-2}]. Ge δ layers were grown by molecular-beam epitaxy (MBE), surfactant-mediated epitaxy (SME),[8–10] and solid-phase epitaxy (SPE). Growth temperature varied from 20 °C (room temperature) to 700 °C.

II. EXPERIMENTAL

For substrate, *n*-type Si (10 mΩ cm) was used. Sample preparation was accomplished in an UHV system equipped with *e*-beam evaporators for Ge and Si and a Knudsen cell for Sb deposition at a base pressure below 1×10^{-10} mbar. Si(111)-7×7 was prepared by short annealing at about 1200 °C for approximately 20 s. Substrate preparation, Ge growth, and subsequent Si deposition was monitored *in situ* by SPALEED, i.e., the 00-beam LEED intensity was measured as a function of coverage. Details on the experimental setup and SPALEED analysis[11,12] have been published elsewhere. Ge flux was calibrated employing SPALEED oscillations during surfactant-mediated growth of a thick Ge film.[10] Ge and Si growth rates were 0.25 BL/min and 1–2 BL/min, respectively. Calibration of Ge flux is estimated to be accurate within ±0.025 BL. Ge deposition was followed by growth of 30 BL Si, sufficiently thick for protection of the Ge layer against oxidation during air transfer and in air XSW measurements. After growth, samples were transferred in air to a XSW stage (ROEMO I) at HASYLAB for characterization of the buried Ge layer. A comparison of LEED results and XSW data was used to determine the change of the Ge distribution during Si deposition. Details on the technique of XSW and data evaluation can be found in the literature.[13,14,7]

III. SPALEED RESULTS

SPALEED was used to characterize the Ge layer during growth. Figure 1 shows the LEED intensity of the 00 beam as a function of deposited Ge and Si during growth by MBE at 490 °C for 0.5, 1, and 1.5 BL total Ge film thickness. At the chosen electron energy, electrons diffracted from adjacent bilayer levels interfere destructively. Therefore, a decrease of 00-beam intensity is directly correlated to the formation of Ge terraces or islands of bilayer height on the Si substrate.[15] Because Ge has the lower surface free energy it wets the Si substrate, while Si does not wet a Ge substrate and forms islands instead. The first oscillation maximum (and, thus, the first nearly smooth and continuous Ge film), however, appears after deposition of 2 BL (Ge+Si)— not 1 BL, independent of the Ge film thickness. Thus, it is concluded that the full first Ge layers grow in a double bilayer fashion as already found for Si homoepitaxy.[12,16] Thus, the Ge film is not completely covering the Si surface up to a coverage of 2 BL. Figure 2 shows a Si substrate covered by a Ge island partially of double bilayer thickness. Initial growth of Ge on Si is not studied here in detail, the pronounced loss of intensity during initial Ge deposition (below 0.1 ML) can be regarded as a hint for a different growth mechanism in this regime.[17]

Growth of Si on bulk Ge is known to proceed in Volmer-Weber mode; immediately forming Si islands instead of a continuous Si film.[18] The observation of intensity oscillations during Si deposition on the Ge clearly reveals a bilayer-by-bilayer growth mode of the Si on the thin Ge films. This is in contrast to results on bulk Ge and thicker Ge films,[19] where Si islanding was found instead of continuous film formation. An oscillation period of 1 BL indicates the typical bilayer growth on the (111) face and the absence of monolayer steps on the surface. Thus, on thin strained Ge films, Si growth by MBE at 490 °C proceeds in bilayer-by-bilayer growth mode.

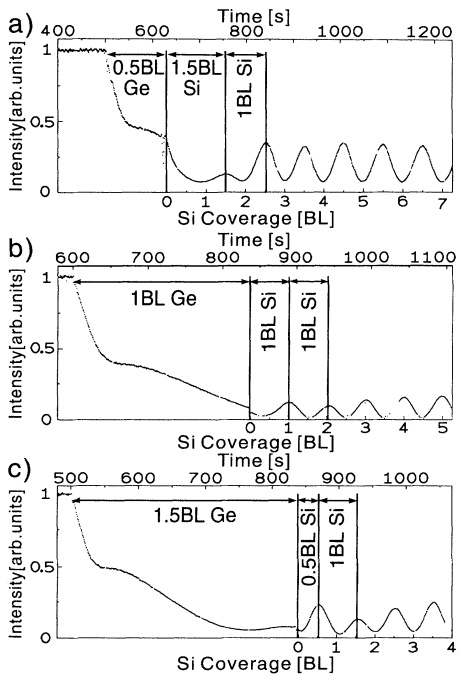

FIG. 1. 00-beam LEED intensity as function of total coverage (Ge+Si) during MBE growth of Si/Ge/Si(111) at 490 °C (a) 0.5 BL Ge, (b) 1 BL Ge, (c) 1.5 BL Ge. The thickness of the Si capping layer is 30 BL.

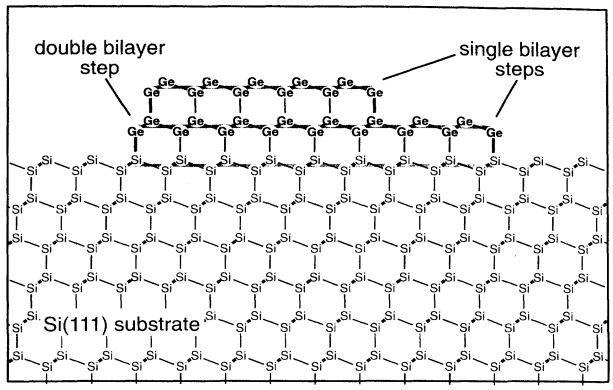

FIG. 2. Schematic view of Ge double bilayer growth on Si(111): Si is covered with a Ge island, partially consisting of a double bilayer Ge. Steps of bilayer and double bilayer height are also indicated.

Using kinematic approximation, LEED intensity was modeled[12] as a function of total thickness (Ge+Si), deriving the Ge layer distribution, which is given in Table I for various growth conditions. For all three Ge films the Ge film is extending over at least 2 BL of thickness, which is not at all a Ge δ layer. The reason for the preferential growth in the second BL is the increased number of nucleation sites compared with the Si substrate due to surface defects as domain boundaries, different superstructure, and irregular step edges.[12]

Figure 3 displays LEED intensity during SME at 700 °C. Ge and Si growth is preceded by adsorption of 1-ML Sb and accompanied by an Sb flux to avoid Sb depletion due to desorption. Again oscillations of the 00-beam LEED intensity are observed. During MBE at 700 °C, without a surfactant, a constant (00)-spot intensity and the absence of intensity oscillations reflect growth in the step-flow mode, i.e., the diffusion length of adatoms

TABLE I. Distribution of Ge to bilayer levels after deposition of 0.5-BL Ge at different growth conditions, p_0: Ge content of top substrate bilayer, p_1 and p_2: Ge content of first and second bilayer level, respectively. The accuracy is about 0.04 BL.

	MBE 490 °C	SME 700 °C	SPE 600 °C
p_0 (BL)		0.3	
p_1 (BL)	0.7	0.6	0.7
p_2 (BL)	0.3	0.1	0.3

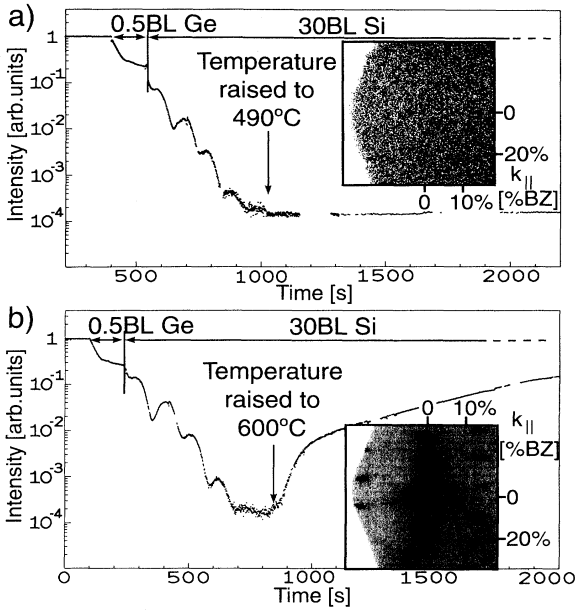

FIG. 3. 00-beam LEED intensity as a function of total coverage (Ge+Si) during SME growth of Si/Ge/Si(111) at 700 °C for a Ge film thickness of 1 BL. The thickness of the Si capping layer is 30 BL.

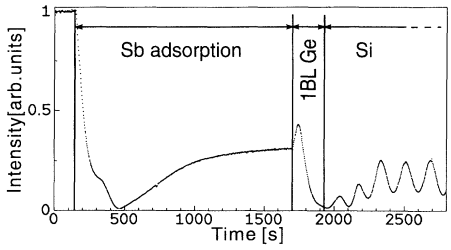

FIG. 4. 00-beam LEED intensity as a function of total coverage (Ge+Si) during SPE growth of Si/Ge/Si(111) at (a) 490 °C and (b) 600 °C. The thickness of the Si capping layer is 30 BL.

is sufficiently large that all deposited atoms nucleate on step sites, which are energetically favorable to island formation on the terraces between steps. Therefore, the average surface morphology does not change with deposition and no change of LEED intensity is observed. Thus, adsorption of Sb reduces the mobility of the adatoms and thus, changes the growth mode from step flow to layer-by-layer growth even at 700 °C.

The first intensity maximum appears after deposition of 0.2 BL Ge. Within kinematic approximation, an increase of 00-beam intensity implies smoothing of a surface. We attribute the initial roughness of the Si substrate to the adsorption process of Sb replacing the Si adatoms of the (7×7) reconstruction, which are rearranged in small islands.[20] During Ge deposition, Sb is exchanged for Ge leaving behind Ge in the top substrate layer (see Table I). Again, a rough Ge film [low (00)-spot intensity] is observed after deposition of 1 BL. With deposition of Si, this roughness is smoothed out again. This is seen in the small change of oscillation period for the first two oscillations during Si deposition and the increase in intensity up to the third oscillation maximum.

SPE is an alternative approach for δ layer formation. Deposition of Ge and topping Si at low temperatures is expected to suppress interdiffusion of Ge and Si during deposition. Unfortunately, low-temperature growth results in formation of crystalline defects, i.e., atoms on nonlattice sites or an amorphous film.[21] Therefore, post-growth annealing is necessary for recrystallization. SPE samples were prepared by deposition of 0.5 BL Ge at room-temperature (RT), followed by 5 BL Si at RT and 25 BL Si at either 490 °C or 600 °C. The LEED intensity as function of total coverage is shown in Fig. 4 along with the observed LEED pattern after completion of growth. The difference is striking. A dramatic loss of intensity is found during RT deposition (note the logarithmic scaling here). No recrystallization is found for 490 °C and no LEED pattern is observed after growth. After annealing at 600 °C, a strong recovery of LEED intensity and a (7×7)+(5×5) LEED pattern is found. Interestingly, coexistence of (7×7) and (5×5) in MBE of Si on Si(111) is found at lower growth temperatures only. After MBE at 600 °C only (7×7) and no (5×5) has been observed.[12] This points to an enhanced defect density of the recrystallized film and surface.

IV. XSW RESULTS

For air transfer, the Ge δ layer is protected against oxidation by the 30 BL Si buffer layer. XSW measurements of the buried Ge film were performed to investigate changes of the layer distribution during Si deposition or post-growth annealing of the Ge film. This allows conclusions on Si-Ge site exchanges, which are caused by intermixing of the species or segregation of the Ge. These processes may affect the abruptness of the desired structure. The changes of the layer distribution were extracted by a comparison of the XSW data to the SPALEED data, which were collected prior to Si deposition.

For XSW, a standard nondispersive setup with a double-crystal monochromator employing a combination of symmetric Ge(111) and asymmetric Si(111) was used at an energy of 12 keV. Sweeping the incidence angle at the sample through Bragg condition, the rocking curve and Ge K_α fluorescence was monitored simultaneously. Coherent position Φ_c and coherent fraction f_c of Ge were extracted from the data by fitting reflectivity and fluorescence to expressions derived from the dynamical theory of x-ray diffraction.[22,23] For the case of all atoms occupying identical sites, the coherent position (or phase) gives the relative position of the fluorescing atoms within the set of substrate lattice planes employed for Bragg diffraction. For cases with atoms on different sites, the coherent position is determined by a weighted average of these sites (see Refs. 13 and 7). The dimensionless parameter Φ_c ranges from 0 to 1 (other values are to be regarded as modulo 1). Coincidence with the substrate lattice planes is indicated by exactly 0 or 1. The coherent fraction f_c is a measure for the spread of the distribution of

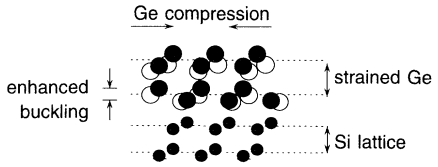

FIG. 5. Schematic view of the Si(111) bilayer: Si atoms are indicated by small symbols, strained Ge by large, and bulklike Ge is shown by open circles. Distances and angles are exaggerated for clarification. Dashed lines show bulklike Si-Si lattice planes and lattice planes of a strained Ge layer. Compressive lateral strain of the Ge layer results in relaxation by enhanced buckling and vertical lattice expansion.

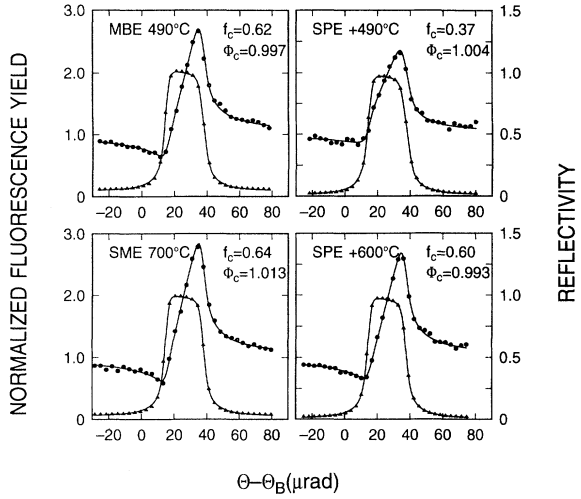

FIG. 6. XSW data for Si/Ge/Si(111): Normalized fluorescence yield (circles) and reflectivity (triangles) as function of angular difference to Bragg condition. Symbols show data points, lines the best fit. (a) 1 BL Ge grown by MBE at 490 °C, 1 BL Ge grown by SME at 700 °C, 0.5 BL Ge grown by SPE and annealed at 490 °C and 600 °C, respectively. (b) 0.5 BL Ge grown by SPE and annealed at 490 °C (open symbols) and 600 °C (filled symbols).

fluorescing atoms around the coherent position. A coherent fraction of 1 indicates that all atoms reside on the corresponding coherent position. In the case of diamond (111), a perfect crystal shows a coherent fraction of 0.707 due to the buckling of the (111) bilayer (see Fig. 5). Details concerning XSW data analysis can be found in the literature.[13,7]

Figure 6 shows reflectivity and normalized fluorescence data for 0.5–1 BL Ge embedded in Si(111) grown under different growth conditions along with the best fit. For 1 BL Ge grown by SME at 700 °C the coherent fraction and coherent position are $f_c=0.64$ and $\Phi_c=1.01$. Taking into account a Debye-Waller factor of 0.987 for bulk Ge[24] this corresponds to an enhanced "buckling" of the Ge bilayer of 6%. Statistical fluctuations were minimized by long data collection times leading to error estimates of $f_c=f_c\pm0.01$ and $\Phi_c=\Phi_c\pm0.005$ for the relative comparison of data within this study. We estimate the absolute accuracy to $f_c=f_c\pm0.02$ and $\Phi_c=\Phi_c\pm0.01$ (0.03 Å). The results for different sample preparations are summarized in Table II.

For interpretation, a model of a laterally compressed Ge layer was used. Because no dislocations are present in these embedded thin Ge films,[9,25] the Ge laterally resides on Si lattice sites and strain relaxation can only occur in the growth direction. This tetragonal distortion was modeled by a shift of the Ge bilayers with respect to Si bilayers and an enhanced buckling of Ge bilayers, i.e., a wider spread of the bilayer (see Fig. 5).

Assuming an incompressible material, an increase of the layer distance is expected for a lateral compression, which occurs during the pseudomorphic growth. The Poisson ratio v describes how compressible a material is. A value of 0.5 is incompressible, a value of 0 is totally compressible. Assuming a Poisson ratio of $v=0.25$,[26] an increase of the layer distance of 6.3% (compared with the Ge bulk value) is expected. For a film with Ge equally distributed to the upper and lower half of its bilayer levels (as measured with LEED prior to Si buffer growth), a coherent position of $\Phi_c>1.03$ is expected. For MBE-SME-, and SPE-grown Ge films with a thickness up to 1 BL, a coherent position of $\Phi_c=0.98$ to 1.01 is found (Table II), pointing to pronounced occupation of the lower half of bilayer levels. Apparently the occupation of the upper and lower bilayer levels with Ge must be changing during Si growth. As a starting point for determination of the Ge distribution after Si growth, the LEED results of Ge bilayer occupation (Table I) were used. Agreement with the XSW data was achieved by Ge-Si site exchanges in upper bilayer levels during initial Si growth. In the model, Ge located in the top half of the surface bilayer was allowed to swap site with Si adatoms. Ge of deeper layers including the lower half of the sur-

TABLE II. Coherent fraction f_c and coherent position Φ_c for different growth methods, substrate temperatures (T), and Ge film thicknesses (Θ).

	MBE		SME		SPE	
T(°C)	490	490	700	700	490	600
Θ (BL)	0.5	1.0	0.5	1	0.5	0.5
f_c	0.62	0.62	0.64	0.64	0.37	0.60
Φ_c	0.98	1.00	0.99	1.01	1.00	0.99

face bilayer was regarded as fixed to its site. The exchange probability was calculated such that the measured coherent fraction was reproduced. Within this model, we find a strong dependence of site-exchange probability on growth conditions. In MBE, about 70% of the surface Ge exchange site with impinging Si adatoms during growth. SPE at room temperature with subsequent annealing reduces site exchange to 40–50 %. SME leads to strongest suppression of site exchanges: Only ~20% of the surface Ge is exchanged for Si during buffer-layer deposition. We regard strain as the driving force for Si-Ge site exchanges as already reported for Ge on Si(001).[27] An alternative view is the concept of surface free energy: during deposition of Si on Ge/Si, Ge segregates to the surface since it lowers the surface free energy of the system Si+Ge/Si(111), explaining the stronger intermixing of Si and Ge. Sb as a surfactant strongly hinders the intermixing of the species because the Ge in a subsurfactant site is nearly immobile and cannot exchange site with Si.[28–31]

Ge-Si intermixing may also affect the wetting ability of subsequently deposited Si on the Ge layer. This may explain why we have observed the wetting of the Ge δ layers with Si instead of the Vollmer-Weber mode (islanding) known from literature. On the other hand, Ge films below 2 BL thickness are not continuous, which may be of importance for nucleation and growth of Si on Ge.

As discussed above, the crystalline quality of room-temperature SPE depends strongly on the post-growth annealing temperature. A small modulation of the fluorescence signal for SPE annealed at 490 °C indicates a small coherent fraction, i.e., a high fraction of Ge atoms on nonlattice sites. After annealing at 600 °C, the coherent fraction is comparable to SME-grown Ge films, indicating effective recrystallization.

V. CONCLUSIONS

Deposition of thin Ge films by MBE, SME, and SPE leads to formation of Ge-Si interfaces of high crystalline quality. SPE requires annealing temperatures higher than $T > 490$ °C for sufficient recrystallization and removal of room-temperature growth defects. Unlike growth on Ge substrates, deposition of Si on thin-strained Ge layers results in a layer-by-layer growth mode—with surfactant (SME at 700 °C) and without surfactant (MBE at 490 °C). For MBE, SME, and SPE, the minimum thickness of a continuous Ge δ layer seems restricted to two bilayers, due to a double bilayer growth mode found for all growth conditions. Growth mode of initially deposited Ge is dominated by nucleation on defects in the growing layer as found for homoepitaxy of Si(111).[12] However, double bilayer growth for Ge on Si(1110 is not as pronounced as for Si on Si(111). Ge-Si site exchanges during growth result in substantial intermixing at the interface and limit achievable abruptness of Ge δ layers. The use of a surfactant strongly reduces the intermixing and allows us to grow abrupt Ge-Si interfaces.

[1]R. D. Barlow, M. G. Dowsett, H. S. Fox, R. A. A. Kubiak, and S. M. Newstead, Nucl. Instrum. Methods Phys. Res. Sect. B **72**, 442 (1992).

[2]F. H. Baumann, M. Bode, Y. Kim, and A. Ourmazd, Utramicroscopy **47**, 167 (1992).

[3]C. van Opdorp, L. J. van IJzendoorn, C. W. Fredriksz, and D. J. Gravesteijn, J. Appl. Phys. **72**, 4047 (1992).

[4]J. F. van der Veen, Surf. Sci. Rep. **5**, 199 (1985).

[5]R. M. Tromp, M. Copel, M. C. Reuter, M. Horn von Hoegen, J. Speidell, and R. Koudis, Rev. Sci. Instrum. **62**, 2679 (1991).

[6]C. Giannini, L. Tapfer, S. Lagomarsino, J. C. Boulliard, A. Taccoen, B. Capelle, M. Ilg, O. Brandt, and K. H. Ploog, Phys. Rev. B **48**, 11 496 (1993).

[7]J. Zegenhagen, Surf. Sci. Rep. **18**, 199 (1993).

[8]M. Copel, M. C. Reuter, E. Kaxiras, and R. M. Tromp, Phys. Rev. Lett. **63**, 632 (1989).

[9]M. Horn von Hoegen, F. K. LeGoues, M. Copel, M. C. Reuter, and R. M. Tromp, Phys. Rev. Lett. **67**, 1130 (1991).

[10]See, M. Horn von Hoegen, M. Pook, A. Al Falou, B. H. Müller, and M. Henzler, Surf. Sci. **284**, 53 (1993), and references therein.

[11]M. Henzler, Appl. Phys. A **34**, 205 (1984).

[12]M. Horn von Hoegen, J. Falta, and M. Henzler, Thin Solid Films **183**, 213 (1989).

[13]M. J. Bedzyk and G. Materlik, Phys. Rev. B **32**, 6456 (1986).

[14]J. Zegenhagen, G. Materlik, and W. Uelhoff, J. X-Ray Sci. Technol. **2**, 214 (1990).

[15]R. Altsinger, H. Busch, M. Horn, and M. Henzler, Surf. Sci. **200**, 235 (1988).

[16]M. Horn von Hoegen and H. Pietsch, Surf. Sci. Lett. **321**, L129 (1994).

[17]B. N. Dev, G. Materlik, F. Grey, R. L. Johnson, and M. Clausnitzer, Phys. Rev. Lett. **57**, 3058 (1986).

[18]P. M. J. Maree, K. Nakagawa, F. M. Mulders, J. F. van der Veen, and K. L. Kavanagh, Surf. Sci. **191**, 305 (1987).

[19]M. Horn von Hoegen, M. Copel, J. C. Tsang, M. C. Reuter, and R. M. Tromp, Phys. Rev. B **50**, 10 811 (1994).

[20]G. Meyer (private communication).

[21]J. Falta and M. Henzler, Surf. Sci. **269/270**, 14 (1992).

[22]M. von Laue, *Röntgenstrahlinterferenzen,* 3rd ed. (Akademische Verlagsgesellschaft, Leipzig, 1960).

[23]B. W. Batterman and H. Cole, Rev. Mod. Phys. **36**, 681 (1964).

[24]M. J. Bedzyk and G. Materlik, Phys. Rev. B **31**, 4110 (1985).

[25]J. W. Matthews and A. E. Blakeslee, J. Cryst. Growth **29**, 273 (1975).

[26]W. A. Brantley, J. Appl. Phys. **44**, 534 (1973).

[27]R. M. Tromp, Phys. Rev. B **47**, 7125 (1993).

[28]W. Dondl, G. Lütjering, W. Wegscheider, J. Wilhelm, R. Schorer, and G. Abstreiter, J. Cryst. Growth **127**, 440 (1993).

[29]P. C. Zalm, G. F. A. van de Walle, D. J. Gravesteijn, and A. A. van Gorkum, Appl. Phys. Lett. **55**, 2520 (1989).

[30]S. Fukatsu, K. Fujita, H. Yaguchi, Y. Shiraki, and R. Ito, Surf. Sci. **267**, 79 (1992).

[31]S. Fukatsu, N. Usami, K. Fujita, H. Yaguchi, Y. Shiraki, and R. Ito, J. Cryst. Growth **127**, 401 (1993).

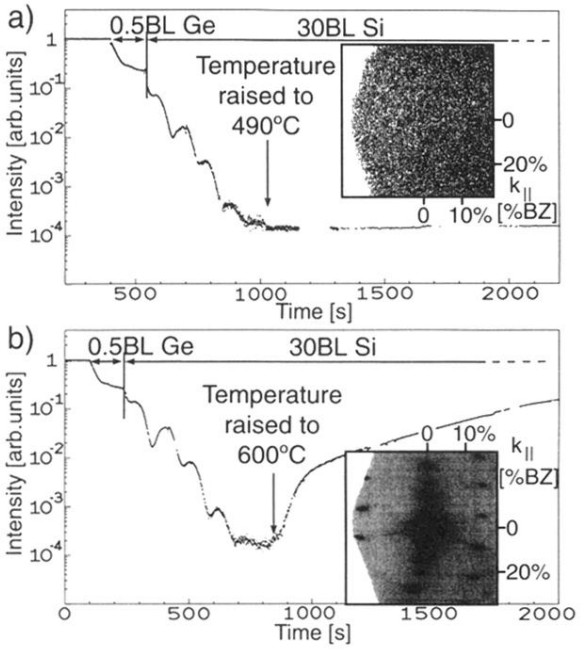

FIG. 3. 00-beam LEED intensity as a function of total coverage (Ge+Si) during SME growth of Si/Ge/Si(111) at 700 °C for a Ge film thickness of 1 BL. The thickness of the Si capping layer is 30 BL.